Micro/Nano Scale Amorphization of Silicon by Femtosecond Laser Irradiation

Amirkianoosh Kiani
Ryerson University

Krishnan Venkatakrishnan
Ryerson University

Bo Tan
Ryerson University

Please Cite:
Kiani, A., Venkatakrishnan, K., & Tan, B. (2009). Micro/nano scale amorphization of silicon by femtosecond laser irradiation. *Optics Express, 17*(19), 16518-16526.
doi:10.1364/OE.17.016518

Micro/nano scale amorphization of silicon by femtosecond laser irradiation

Amirkianoosh Kiani,[1] Krishnan Venkatakrishnan,[1] Bo Tan[2,*]

[1]*Department of Mechanical and Industrial Engineering, Ryerson University, 350 Victoria Street, Toronto, ON, Canada M5B 2K3*

[2]*Department of Aerospace Engineering, Ryerson University, 350 Victoria Street, Toronto, ON, Canada M5B 2K3*

**tanbo@ryerson.ca*

Abstract: This research aimed to investigate the feasibility of using direct amorphization of silicon induced by femtosecond laser irradiation for maskless lithography. A thin layer of amorphous silicon of predetermined pattern was first generated by irradiation by a femtosecond laser of Mega Hertz pulse frequency. The following KOH etching revealed that the amorphous silicon layer acted as an etch stop. Line width less than 1/67 the focused spot size was demonstrated and hence the proposed maskless lithography process has the potential of producing submicron and nanoscale features by employing a laser beam of shorter wavelength and a high NA focusing lens. Scanning Electron Microscope (SEM), a Micro-Raman and Energy Dispersive X-ray (EDX) spectroscopy analyses were used to evaluate the quality of amorphous layer and the etching process.

OCIS codes: (140.3390) Laser materials processing; (140.6810) Thermal effects; (350.5340) Photothermal effects; (110.5220) Photolithography; (320.7090) Ultrafast lasers; (160.6000) Semiconductor materials.

References and links

1. D. Bauerle, *Laser processing and chemistry*, (Springer, New York, 3rd ed., 2000).
2. D. Lim, Y. Kamotani, B. Cho, J. Mazumder, and S. Takayama, "Fabrication of microfluidic mixers and artificial vasculatures using a high-brightness diode-pumped Nd:YAG laser direct write method," Lab Chip **3**(4), 318–323 (2003).
3. B. Tan, A. Dalili, and K. Venkatakrishnan, ""High Repetition Rate Femtosecond Laser Nano-machining of Thin Films," J," Appl. Phys., A Mater. Sci. Process. **95**(2), 537–545 (2009).
4. P. Stanley, K. Venkatakrishnan, and L. E. N. Lim, "Direct writing of photomask by ultrashort laser," J. Vac. Sci. Technol. B **21**(1), 204–206 (2003).
5. K. Venkatakrishnan, B. K. A. Ngoi, P. Stanley, L. E. N. Lim, B. Tan, and N. R. Sivakumar, "Laser writing techniques for photomask fabrication using a femtosecond laser," Appl. Phys., A Mater. Sci. Process. **74**(4), 493–496 (2002).
6. H. Yasuda, S. Arai, J. Kai, Y. Ooae, T. Abe, S. Maruyama, and T. Kiuchi, "Multielectron beam blanking aperture array system SYNAPSE-2000," J. Vac. Sci. Technol. B **14**(6), 3813–3820 (1996).
7. B. Schmidt, L. Bischoff, and J. Teichert, "Writing FIB implantation and subsequent anisotropic wet chemical etching for fabrication of 3D structures in silicon," Sens. Actuators A Phys. **61**(1-3), 369–373 (1997).
8. J. A. Dagata, J. Schneir, H. H. Harary, C. J. Evans, C. J. Postek, and J. Bennett, "Modification of hydrogen-passivated silicon by a scanning tunnelling microscope operating air," Appl. Phys. Lett. **56**(20), 2001–2003 (1990).
9. S. C. Minne, H. T. Soh, P. Flueckinger, and C. F. Quate, "Fabrication of 0.1-MU-M Metal-Oxide-Semiconductor Field-Effect Transistors with the atomic-force microscope," Appl. Phys. Lett. **66**(6), 703–705 (1995).
10. P. M. Chapbell, E. S. Snow, and P. J. McMarr, "Fabrication of nanometer-scale side-gated silicon field-effect transistors with an atomic-force microwave," Appl. Phys. Lett. **66**(11), 1388–1390 (1995).
11. F. S. S. Chien, C. L. Wu, Y. C. Chou, T. T. Chen, S. Gwo, and W. F. Hsieh, "Nanomachining of (110)-oriented silicon by scanning probe lithography and anisotropic wet etching," Appl. Phys. Lett. **75**(16), 2429–2431 (1999).
12. Y. Y. Zhang, J. Zhang, G. Luo, X. Zhou, G. Y. Xie, T. Zhu, and Z. F. Liu, "Fabrication of silicon-based multilevel nanostructures via scanning probe oxidation and anisotropic wet etching," Nanotechnology **16**(4), 422–428 (2005).
13. K. Ueno, R. Okada, K. Saiki, and A. Koma, "Nano-scale anodic oxidation on a Si(111) surface terminated by bilayer-GaSe," Surf. Sci. **514**(1-3), 27–32 (2002).

#114668 - $15.00 USD Received 22 Jul 2009; revised 10 Aug 2009; accepted 12 Aug 2009; published 1 Sep 2009

14. F. S. S. Chien, J. W. Chang, S. W. Lin, Y. C. Chou, T. T. Chan, S. Gwo, T. S. Chao, and W. F. Hsieh, "Nanometer-scale conversion of Si3N4 to SiOx," Appl. Phys. Lett. **76**(3), 360–362 (2000).
15. D. A. Weinberger, S. Hong, C. A. Mirkin, B. W. Wessels, and T. B. Higgins, ""Combinatorial generation and analysis of nanometer- and micrometer-scale silicon features via "dip-pen" nanolithography and wet chemical etching," Adv. Mater. **12**(21), 1600–1603 (2000).
16. H. T. Lee, J. S. Oh, K. H. Park, J. S. Ha, H. J. Yoo, and J. Y. Koo, "Nanometer-scale lithography on H-passivated Si(100) by atomic force microscope in air," J. Vac. Sci. Technol. A **15**(3), 1451–1454 (1997).
17. N. Kawasegi, N. Morita, S. Yamada, N. Takano, T. Oyama, and K. Ashida, "Etch stop of silicon surface induced by tribo-nanolithography," NanoBiotechnology **16**, 1411–1414 (2005).
18. J. W. Park, N. Kawasegi, N. Morita, and D. W. Lee, "Tribonanolithography of silicon in aqueous solution based on atomic force microscopy," Appl. Phys. Lett. **85**(10), 1766–1768 (2004).
19. J. W. Park, N. Kawasegi, N. Morita, and D. W. Lee, ""Mechanical approach to nanomachining of silicon using oxide characteristics based on tribo nanolithography (TNL) in KOH solution," ASME," J. Manuf. Sci. Eng. **126**(4), 801–806 (2004).
20. K. Venkatakrishnan, B. Tan, P. Stanely, L. E. N. Lim, and B. K. A. Ngoi, "Femtosecond pulsed laser direct writing system," Opt. Eng. **41**(6), 1441–1445 (2002).
21. J. M. Liu, R. Yen, H. Kurz, and N. Bloembergen, "Phase-Transformation on and charged-partocle emisson from a silicon crystal-surface, induced by picosecond laser-pulses," Appl. Phys. Lett. **39**(9), 755–757 (1981).
22. J. Bonse, S. Baudach, J. Kruger, W. Kautek, and M. Lenzner, "Femtosecond laser ablation of silicon-modification thresholds and morphology," Appl. Phys. A Mater. Sci. Process. **74**, 19–25 (2002).
23. C. C. Bradley, W. R. Anderson, J. J. McClelland, and R. J. Celotta, "Nanofabrication via atom optics," Appl. Surf. Sci. **141**(3-4), 210–218 (1999).
24. A. V. Osipov, P. Patzner, and P. Hess, "Kinetics of laser-induced oxidation of silicon near room temperature," Appl. Phys., A Mater. Sci. Process. **82**(2), 275–280 (2006).
25. P. Patzner, A. V. Osipov, and P. Hess, "Photoinduced self-limited low-temperature growth of ultra-thin silicon-oxide films with water vapor," Appl. Phys., A Mater. Sci. Process. **85**(2), 145–150 (2006).
26. J. Bonse, K. W. Brzezinka, and A. J. Meixner, "Modifying single-crystalline silicon by femtosecond laser pulses: an analysis by micro Raman spectroscopy, scanning laser microscopy and atomic force microscopy," Appl. Surf. Sci. **221**(1-4), 215–230 (2004).

1. Introduction

Photolithography is the most widely used technique to fabricate microelectronics, microelectromechanical and nanoelectromechanical systems (MEMS and NEMS), microstructures for microfluidic systems as devices for chemistry and biochemistry, Lab On a Chip system (LOC) and other applications [1,2]. This technique requires a photomask for replication. The fabrication of photo masks are normally very expensive (up to $100K per piece) and time consuming due to the fact that there are several steps involved in the fabrication process [3–5]. Therefore, photolithography is only cost efficient for high volume mass production. With the trend of semiconductor manufacturing moving towards customization, small volume fabrication is becoming more and more popular. The customized production in turn resulted in growing interest in maskless lithography that can significantly reduce the cost of prototyping and manufacturing.

Several approaches have been proposed for maskless lithography [6–19], among which techniques that based on atomic force microscopy are the most widely investigated. These techniques include scanning probe oxidation [8–16], Tribo nanolithography (TNL) [17–19] and dip-pen lithography (DPL) [15]. A common characteristic of these techniques is that they all involve two steps: first, the scanning probe either deposits or directly induces a thin layer of etch stop on the top surface of a silicon substrate; then the following chemical etching reveals the positive or negative features. In the scanning probe oxidation approach and the tribo nanolithography approach, the probe has to be in contact with the silicon substrate in order to generate an oxide or amorphous layer. Normally, a blunt-tipped probe will be employed and a mechanical force in the range of μN must be applied to obtain an etch stop layer of thickness in sub-10 nm range. Due to the contact nature of these approaches, the minimum line width is limited by the dimension of the Atomic Force Microscope (AFM) tip, usually in the order of 50 nm. In the case of dip pen nanolithography, line width of 5~15 nm can be achieved since sharper tip can be employed for deposition. For these applications, the velocity of an Atomic Force Microscope (AFM) scanning probe is normally set to be around 300 nm/sec and the scanning field (X × Y) of an AFM is typically around 100 μm × 100 μm.

#114668 - $15.00 USD Received 22 Jul 2009; revised 10 Aug 2009; accepted 12 Aug 2009; published 1 Sep 2009

Thus, it determined that nanolithography approaches that employ AFM are slow processes and only applicable to micron-sized devices. For large scale manufacturing, cell stitch must be performed and it could be very challenging due to the small dimension of each cell.

In this research, we attempted to develop an alternative maskless nanolithography by a combination of femtosecond laser amorphization of silicon and wet etching. Using a high repetition femtosecond laser (MHz) enables us to control laser fluence below ablation threshold which causes crystalline silicon phase transition to an amorphous state. The induced thin layer of amorphous silicon is then used as an etch stop in the following wet chemical etching (KOH) for maskless lithography. This may lead to a promising solution for maskless nanolithography because laser beam is a non-contact probe and can be scanned at very high speed. To the best of our knowledge, we are the first to report direct maskless etch stop writing by amorphization of silicon by high repetition femtosecond laser irradiation for bulk micromaching application.

2. Experimental setup and fabrication process

Figure 1 illustrates the proposed maskless fabrication technique, which combines femtosecond laser irradiation and wet chemical etching. First, silicon wafers are irradiated with femtosecond pulses with pulse energy well below the damage threshold. Then, the treated samples are etched in a KOH solution.

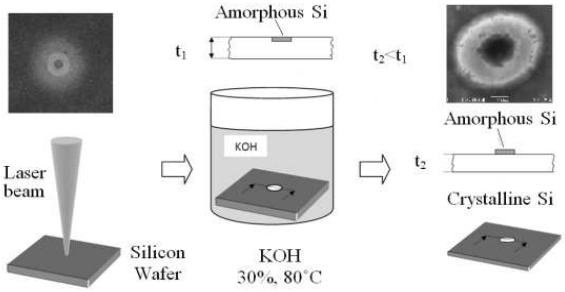

Fig. 1. Process of experiment.

Figure 2 shows schematic drawing of the experimental setup. To study the silicon amorphization, we used undoped <100> oriented silicon wafer. Prior to laser irradiation, the samples were cleaned with alcohol and ultra pure water. The Femtosecond laser used in the study was a diode-pumped, Yb-doped system. The average output power is 11 W with a central wavelength of 1030 nm and a repetition rate ranging between 200 kHz and 26 MHz. This laser emits pulses of 200 fs pulse duration. The diameter of circular output beam from the laser is around 4.5 mm. The laser beam was expanded to 9 mm by a combination of a plano-convex (f = −100) and a plano-concave (f = 200) lenses; then the laser beam was rotated to circularly polarized by a quarter waveplate placed in the beam path. The diameter of beam is reduced to 8mm by using an iris diaphragm before entering to galvo scanner. A two-axis galvo-scanner was used for beam scanning since it has a high scanning speed (to 3000 mm/s). Such a high speed is very difficult to achieve with a mechanical translation stage. In order to focus the normal beam to the surface of silicon, scan lens of a focal length of 63.5 mm was employed. The theoretical focused laser spot diameter (d_0) is calculated from: $d_o \approx 1.27\,\lambda_o F/D$ [20]. Here, F is the effective focal length of the scan lens, λ_o is the wavelength of the laser equal to 1030 nm and D is the laser beam diameter at the input of the galvo-scanner, which is 8 mm. From this formula the theoretical spot size is calculated to be 10.38 μm in diameter. During the experiment the spot size may be bigger due to scatter and misalignment. The average laser fluence was calculated to be 0.15~0.35 J/cm^2 at the repetition rate of 13 and 26 MHz. In the present experiment the dwell time is 0.1 ms and scanning speed of line features is in the range of 100-150 mm/s

#114668 - $15.00 USD Received 22 Jul 2009; revised 10 Aug 2009; accepted 12 Aug 2009; published 1 Sep 2009

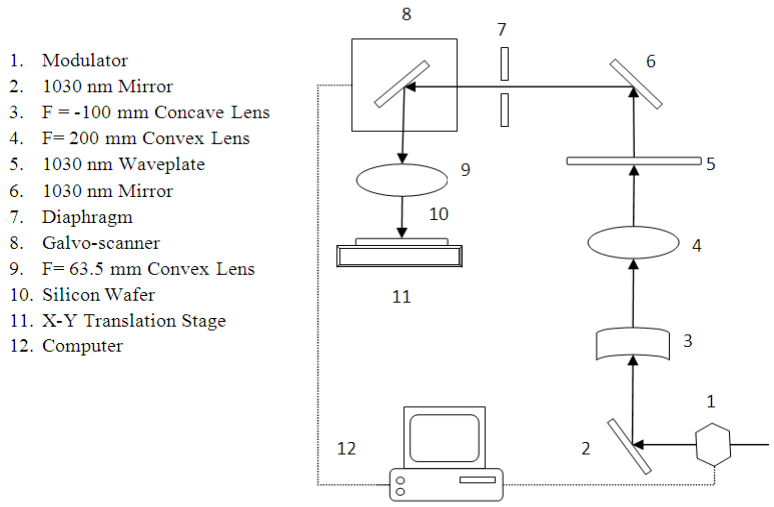

Fig. 2. Experimental Setup.

Etched samples were examined under a Scanning Electron Microscope (SEM), a Micro-Raman and Energy Dispersive X-ray (EDX) spectroscopy to evaluate the quality of amorphous layer and the etching process. Back scattering micro-Raman analysis was performed at room temperature using 532 nm line of Ar ion laser source.

3. Discussion and results

Figure 3(b) shows morphology after irradiation with sub-threshold femtosecond laser pulses. Surface morphologies vary according to the intensity distribution of a Gaussian beam. At the center region where the laser fluence was the highest, ablation occurred, as expected. In this zone the intensity of a Gaussian beam is above the surface damage threshold. Therefore, material removal takes place. The next annulus could be a thin layer of amorphous or polycrystalline silicon because when observed under SEM this region showed a difference in reflectivity. The amorphous phase could be formed on crystalline silicon because of the rapid cooling after the femtosecond excitement, which is up to 10^{13} °C/s [21]. Therefore, there is not enough time for the material to return to the crystalline phase. It is noteworthy that the phase change on crystalline silicon was restricted only within a certain range of laser fluence [21,22]. Above this fluence range, for example, at the center of the Gaussian beam, high pulse energy causes ablation. It was observed that after etching the center zone was removed by etchant. Thus, the central zone was not in amorphous state.

#114668 - $15.00 USD Received 22 Jul 2009; revised 10 Aug 2009; accepted 12 Aug 2009; published 1 Sep 2009

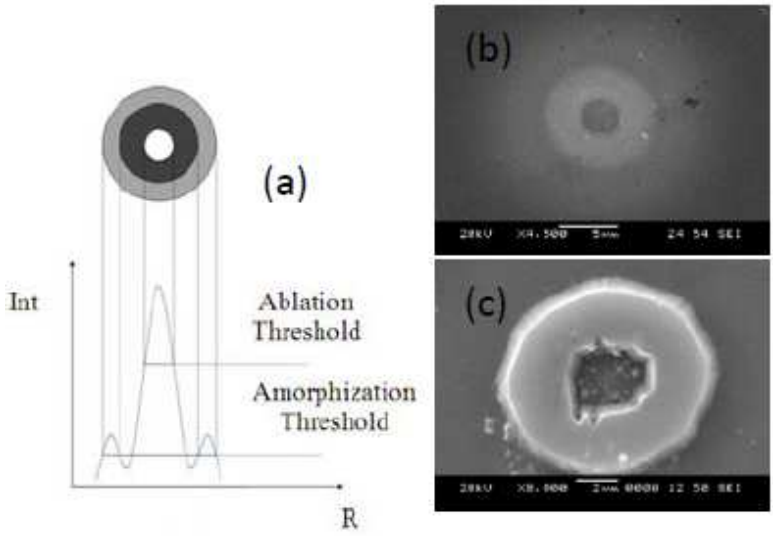

Fig. 3. (a) Schematic drawing of laser intensity and surface modification on silicon substrate. (b) Silicon wafer after irradiation with sub-threshold. (c) Silicon wafer after etching.

In the outermost annulus, we did not expect to see any phase change because the laser energy fluence is lower than the amorphous modification threshold. However, the SEM image (Figure. 3 (b)) shows that outside the unmodified annulus, there was another modified annulus. This annulus can be attributed to the secondary intensity peak generated by diffraction. After etching, this region cannot be seen in the SEM images. Laser energy fluence at the secondary peak was not high enough to completely change the phase of the material. It was only sufficient to slightly modify the material; therefore it was removed in the post-irradiation etching process. After etching, it was observed that the non-irradiated area and the central region of the laser irradiation are etched by KOH; whereas, the annulus around the central region of the laser spot is scarcely etched. Consequently, a ring feature stands out on the etched silicon substrate, suggesting that the amorphous layer resists to KOH. The internal quadrilateral shapes are due to the orientation of the silicon crystal (Fig. 4). This observation is in agreement with the etch rate of amorphous silicon reported by Kawasegi N. et al. [17,19] According to Kawasegi et al, the etch rate of amorphous silicon which formed by magnetron spattering was over 30 times lower than that of crystalline silicon<100>.

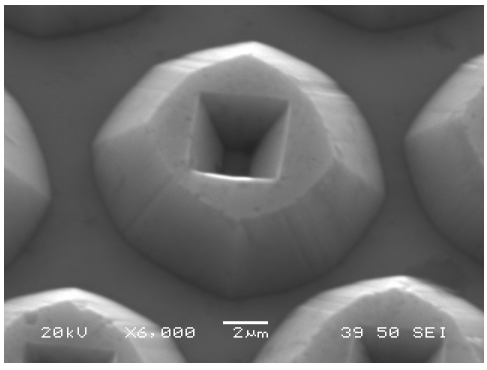

Fig. 4. SEM image of ring feature after etching in KOH solution for 15min at 45°C (Average laser fluence: 0.27 J/cm^2)

A well defined circular dot instead of a ring feature is more applicable in most applications. In order to get a circular dot after wet etch, the intensity of the laser beam should

#114668 - $15.00 USD Received 22 Jul 2009; revised 10 Aug 2009; accepted 12 Aug 2009; published 1 Sep 2009

be controlled such that the peak intensity does not exceed the ablation threshold. Figure 5 gives SEM images of features obtained after wet etching. Round pad was obtained by reducing the pulse energy, as shown in Fig. 5 (b). The pad is around 2 µm in diameter, which is far smaller than the estimated focused laser spot. This demonstrated that the intensity of the laser beam can be accurately controlled such that only a small section surround the central peak of the Gaussian beam is above the amorphization threshold, enabling the creation of features smaller than the focused spot. Using the same technique the authors have created sub-100 nm ablated features with a laser spot of 2 µm diameter in their previous research work [3].

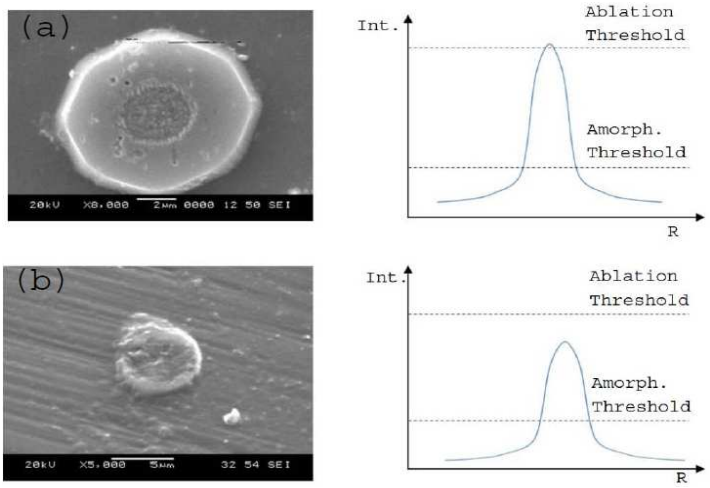

Fig. 5. SEM images features after 3 min etching) (a) ring feature at average laser fluence of 0.3J/cm^2 (b) solid round at 0.2J/cm^2

The fabrication of micro and nanometer-scale lines may be useful for such diverse applications as micro and nano scale length standards, optical grating fabrication, or in the development of novel sensors [23]. Figure 6 presents line features generated with the described maskless lithography. The thickness and width of the induced layer (amorphous layer) were calculated to be approximately 1.4 µm and 6 µm. The average laser fluence was 0.28 J/cm^2 at the repetition rate of 26 MHz. As it was expected, the part of the substrate that was not irradiated with laser beam was dissolved after etching and a pyramid like structure with sidewall slope at 54.74° was formed (See Fig. 6, zone (b)), while, the irradiated zone was not etched in the etchant solution and the angle of sidewall of irradiated zone is 90° (See Fig. 6, zone (a)). It can be concluded from this observation that the irradiated zone is not in crystalline state. Further analyses performed by EDX and Micro-Raman demonstrated that the irradiated zone is silicon in amorphous state rather than crystalline state or silicon oxide.

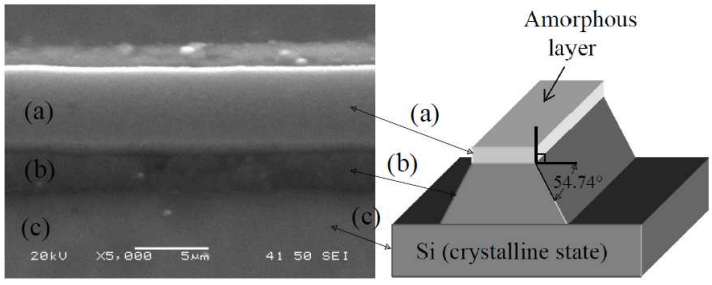

Fig. 6. SEM image (at the incident angle of 35°) of line feature after etching in KOH solution (Pulse energy: 0.28 J/cm^2)

#114668 - $15.00 USD Received 22 Jul 2009; revised 10 Aug 2009; accepted 12 Aug 2009; published 1 Sep 2009

Figure 7 presents line features generated with a scanning laser spot of various pulse energies. As pulse energy reduces the line width reduces. The smallest line width we obtained with the 10 µm laser spot is around 150 nm, as shown in Fig. 7(d). The line width is around 1/67 of the laser spot diameter. Since laser beam can be easily focused down to 1~2 µm with a focusing lens of a high numerical aperture, together with the adoption of laser frequency doubling or tripling, nanoscale feature size can be expected.

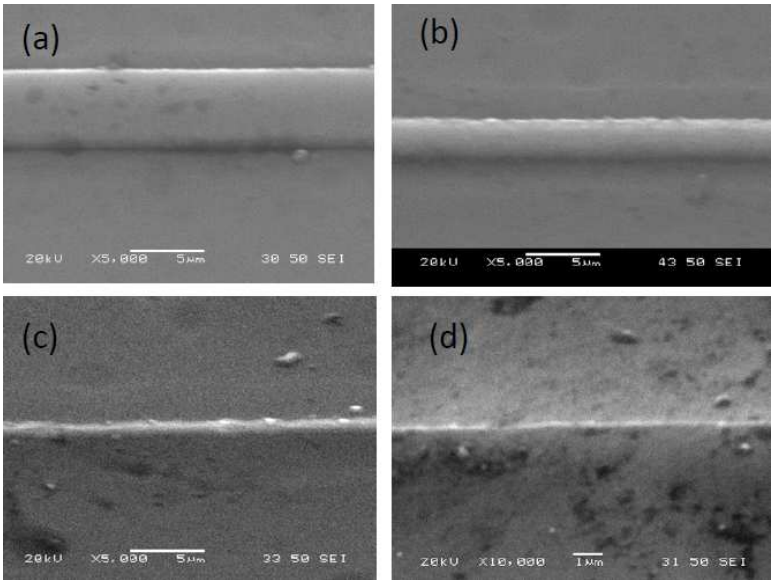

Fig. 7. (a) 5 µm linewidth at pulse energy of 0.28 J/cm^2 (at 26 MHz) (a) 2.5 µm linewidth at pulse energy of 0.24 J/cm^2 (at 26 MHz) (b) 1.0 µm linewidth at pulse energy of 0.2 J/cm^2 (at 26 MHz) (c) 150 nm linewidth at pulse energy of 0.08 J/cm^2 (at 26 MHz)

Investigations done previously indicated that upon sub-damage-threshold laser irradiation on silicon wafers a thin layer on the top surface has been converted to a chemical compound, such as silicon oxide and silicon hydroxide [24,25]. However, this is not the case in our experiment. EDX analysis of the irradiated zone excluded the possibility of compound formation since no trace of oxygen was observed (Fig. 8).

#114668 - $15.00 USD Received 22 Jul 2009; revised 10 Aug 2009; accepted 12 Aug 2009; published 1 Sep 2009

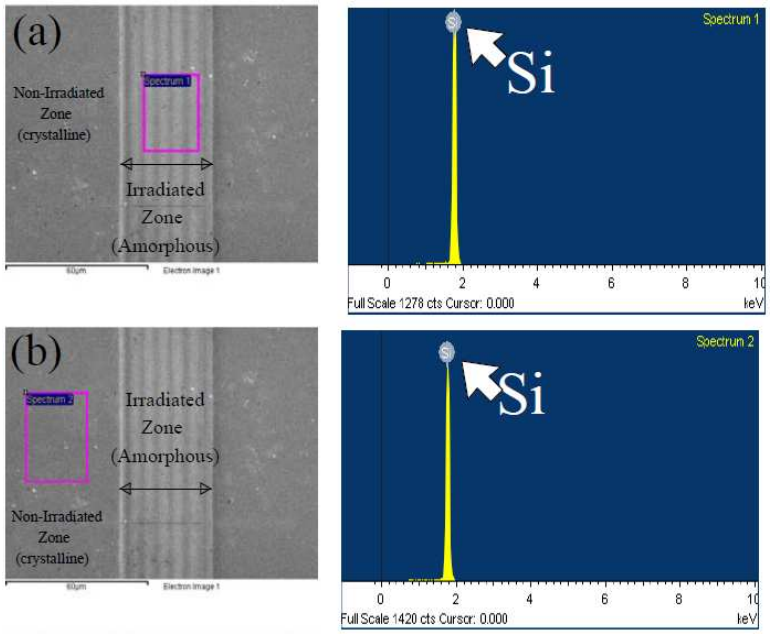

Fig. 8. EDX analysis of (a) irradiated zone and (b) non-irradiated zone

Raman Spectroscopy measurements were performed to study the crystal properties of different zones observed after laser irradiation. Raman spectrum is dominated by the signal at 517 cm^{-1} which corresponds to crystalline silicon. In contrast the broad band observed around 506.9 cm^{-1} is the characteristic for amorphous silicon [26]. Therefore, we conclude that the induced zone is amorphous silicon rather than silicon oxide (Fig. 9).

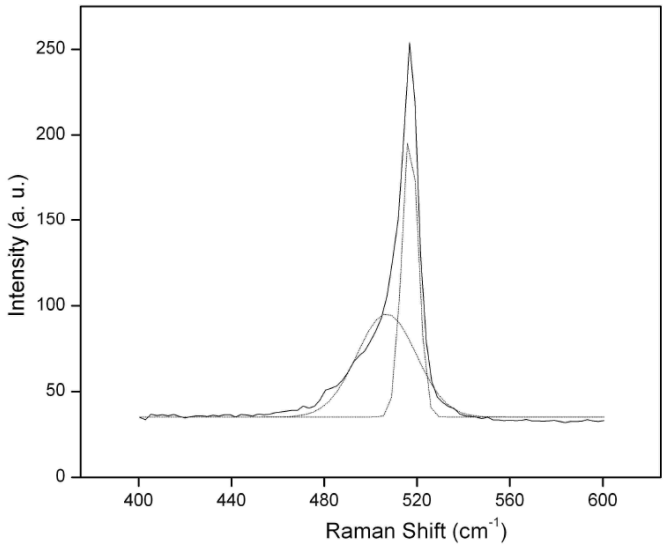

Fig. 9. Raman spectroscopy graph.

Compared with approaches that based on Atomic Force Microscope (AFM), the described method has many advantages. First of all, at 3000 mm/sec probe scanning speed the processing time of patterning is next to zero for a feature with dimension within the scan field. Whereas, it takes a few minutes to complete the patterning if an Atomic Force Microscope

#114668 - $15.00 USD Received 22 Jul 2009; revised 10 Aug 2009; accepted 12 Aug 2009; published 1 Sep 2009

(AFM) is used [18,19]. Secondly, the scanning filed of a laser system is much larger than that of an AFM: 1 mm × 1 mm is normally associated with a 10 μm laser spot. Therefore, sub-millimeter devices can be fabricated without stitch and, for large scale patterning, cell stitch can be performed with more tolerance on misalignment between cells. Finally, due to the non-contact nature of laser probe this process does not suffer issues that normally associated with tools wear

4. Conclusion

In this study, we proposed and demonstrated a new method for maskless fabrication, using a combination of femtosecond pulses laser induced silicon amorphization and wet chemical etching. Amorphous layers formed by laser irradiation acted as an etch stop in KOH and micro and nano-features were fabricated by this method. Scanning Electron Microscope (SEM), a Micro-Raman and Energy Dispersive X-ray (EDX) spectroscopy were employed to evaluate the quality of amorphous layer and the etching process. An important advantage of this technique is the use of femtosecond pulses laser which makes it particularly suitable for rapid prototyping and custom-scale manufacturing for a wide variety of applications in MEMS, NEMS, fabrication of semiconductor and Lab On a Chip systems. We generated features less than 1/67 the focused spot size by controlling the by controlling the laser fluence and etching parameters. Submicron and nanoscale feature size can be expected by reducing the focused spot size and optimizing etching parameters. Moreover, the wet etch process guarantees well defined shape and smooth finishing in the final products. In the future, more investigations will be carried out to control the thickness of the amorphous silicon layer to study its effect on aspect ratio and to reduce the features size in nano-scale by optimizing laser parameters and etching process.

Acknowledgments

This research is funded by Natural Science and Engineering Research Council of Canada.

#114668 - $15.00 USD Received 22 Jul 2009; revised 10 Aug 2009; accepted 12 Aug 2009; published 1 Sep 2009